Friction **9**(3): 513–523 (2021)
https://doi.org/10.1007/s40544-019-0354-7
ISSN 2223-7690
CN 10-1237/TH

RESEARCH ARTICLE

Quantification/mechanism of interfacial interaction modulated by electric potential in aqueous salt solution

Shaowei LI[1], Pengpeng BAI[1], Yuanzhe LI[1], Noshir S. PESIKA[2], Yonggang MENG[1], Liran MA[1,*], Yu TIAN[1,*]

[1] *State Key Laboratory of Tribology, Department of Mechanical Engineering, Tsinghua University, Beijing 100084, China*

[2] *Department of Chemical and Biomolecular Engineering, Tulane University, New Orleans, LA 70118, USA*

Received: 02 September 2019 / Revised: 02 December 2019 / Accepted: 12 December 2019

Abstract: With the development of surface and interface science and technology, methods for the online modulation of interfacial performance by external stimuli are in high demand. Switching between ultra-low and high friction states is a particular goal owing to its applicability to the development of precision machines and nano/micro-electromechanical systems. In this study, reversible switching between superlubricity and high friction is realized by controlling the electric potential of a gold surface in aqueous salt solution sliding against a SiO_2 microsphere. Applying positive potential results creates an ice-like water layer with high hydrogen bonding and adhesion at the interface, leading to nonlinear high friction. However, applying negative potential results in free water on the gold surface and negligible adhesion at the interface, causing linear ultra-low friction (friction coefficient of about 0.004, superlubricity state). A quantitative description of how the external load and interfacial adhesion affected friction force was developed, which agrees well with the experimental results. Thus, this work quantitatively reveals the mechanism of potential-controlled switching between superlubricity and high-friction states. Controlling the interfacial behavior via the electric potential could inspire novel design strategies for nano/micro-electromechanical and nano/micro-fluidic systems.

Keywords: electrochemical potential; reversible switching; superlubricity; nonlinear friction; adhesion

1 Introduction

Researchers have been studying friction for centuries owing to the universality of frictional forces and the massive energy wastage they cause. Friction is generally a comprehensive result of numerous surface asperity collisions at the micro/nanoscale, making it difficult to be accurately predicted and controlled [1–3]. Atomic force microscopy (AFM) is a versatile tool for studying friction mechanisms at the nanoscale, which significantly reduces the complexity of the problem [4–6]. The friction between two solid dry surfaces involves both mechanical resistance [7, 8] and interfacial interaction [9, 10]. Corrugation of the potential energy surface is an essential friction mechanism [11, 12]. It is helpful to reduce the friction between interfaces by maintaining a flat potential energy surface [11, 12]. When a liquid medium is introduced between two solid surfaces, it works as a lubricant to reduce the friction force according to the hydrodynamic effect and/or adsorbed boundary film [13–18]. Water-based lubricants have been widely studied owing to their low viscosity and environmentally friendly properties [19–21]. The application of external fields is also an effective strategy for controlling and regulating interfacial friction [22–24]; the electric potential of a surface can be especially useful for controlling its interfacial friction behavior in solution [4, 25, 26]. Thus, studying the effects of electric potential on friction can aid our understanding of friction mechanisms.

In aqueous solutions, water molecules rearrange their conformations on charged surfaces [27–30], resulting

* Corresponding authors: Liran MA, E-mail: maliran@mail.tsinghua.edu.cn; Yu TIAN, E-mail: tianyu@mail.tsinghua.edu.cn

in viscosities near the surface that are 10^5–10^7 orders of magnitude higher than that of bulk water [31–37]. Previous studies have shown that such confined water layers have a significant impact on the frictional properties of the surface. For example, Dhopatkar et al. [38] reported that, when water is confined between two charged solid surfaces modified with cationic surfactants, it becomes "ice-like" and greatly reduces the interfacial friction between the two surfaces. In contrast, Valtiner et al. [39] studied the friction between mica and gold surfaces in an electrochemical environment, and reported that the highly viscous water layer that formed on the positively charged gold surface increased the interfacial friction. Clearly, the orientation of water molecules under an electric field profoundly affects the friction between surfaces. However, the reasons for this are not yet fully understood. In an attempt to elucidate this phenomenon, Pashazanusi et al. [40] studied the friction between a SiO_2 probe and a gold surface using electrochemical AFM. They noted that the friction force under a positive potential (+0.6 V vs. Ag) was ~35-times higher than that under a negative potential (−0.6 V vs. Ag). These results were attributed to the formation of hydrogen bonds between the SiO_2 probe and the ice-like water layer on the positively charged gold surface. Such hydrogen bond formation was further confirmed by the results of adhesion tests performed by Li et al. [41], who suggested that hydrogen bonds form between hydrophilic SiO_2 microspheres and the ice-like water layer; conversely, hydrophobic polystyrene microspheres form no such bonds owing to the lack of hydroxyl groups on their surfaces.

Previous studies on electrically controlled friction have successfully converted the frictional states of surfaces from low to high (and vice versa) by controlling the adsorption of surfactants [42, 43], the adsorption structure of ionic liquids [26, 44], and the structure of adsorbed water molecules [38–41]. However, changing the surface frictional state between superlubricity (coefficient of friction (CoF): <0.01) and high friction in real-time remains a challenge. With the development of industrial applications that require improved frictional control, strategies for reversibly switching between superlubricity and highly frictional states are in increasing demand [45–47].

Previously [40], the reversible switching of friction forces between an AFM tip and a gold surface was observed upon changing the electric potential. However, since the applied load was relatively large (micronewton magnitude) and the tip was very sharp (radius of curvature: <10 nm), the lowest CoF that could be obtained was still above 0.1. In this study, we used a relatively low load (nanonewton magnitude) and a SiO_2 microsphere tip (radius: 10 μm), which allowed reversible switching between superlubricity and high nonlinear friction by controlling the electric potential of the gold surface in aqueous salt solution electrolyte. In addition, we established a quantitative relationship between adhesion and friction for the boundary lubrication state. Thus, the current work provides new insight into the origins of frictional forces and the physical properties of confined liquid layers on solid surfaces. The findings will aid the design and control of micro/nano-electromechanical systems (M/NEMSs).

2 Experimental section

Preparation of gold film: A grade-V1 mica plate (S & J Trading, Inc.) was cut into 10 mm × 10 mm sheets and cleaved using scotch tape, then immediately placed in a sputtering vacuum chamber (ATC2200-V sputtering system, AJA International, Inc.) to avoid contamination by pollutants in the air. A gold film with a thickness of approximately 100 nm was then deposited on the mica surface. The deposition rate was ~1 Å/s and the vacuum was maintained at 10^{-6} Torr. The gold-coated mica was removed from the chamber and immediately placed into a closed sample box filled with dry nitrogen gas. Prior to conducting the electrochemical and friction experiments, the gold-coated mica was washed with deionized water and dried with nitrogen gas.

Electrochemistry and friction experiments: A SiO_2 microsphere with a diameter of 20 μm was glued onto a tipless AFM cantilever (FORT-TL), which was used to measure the interfacial forces on the charged gold-coated substrates in combination with a Multimode 8 AFM system (Bruker Corporation, Santa Barbara, CA). An AFM tip was used to image the topography of the gold surface. A universal biopotential (Veeco Instruments) was used to control the electric potential of the gold surface, and a 0.1 M NaCl aqueous solution was used as the electrolyte. Ag and Pt wires with diameters of 0.5 mm were used as the quasi-reference

electrode and counter electrode, respectively. The gold surface was used as the working electrode. The potential was limited to between −0.6 and +0.6 V, because the adsorption of ions (e.g., chloride ions) is minimal in this range, and there are no faradaic processes such as gold oxidation [40, 41]. All the electric potentials in this work are given as vs. Ag electrode. When the potential was higher/lower than the potential of zero charge (U_{pzc} = 100 mV), the gold was considered to be positively/negatively charged [41].

The spring constant of the AFM cantilever was calculated by the Sader method [48–50]. The deflection sensitivity was calibrated based on the slope of a retraction force curve obtained by pressing a SiO_2 microsphere glued to a cantilever onto a sapphire wafer. The normal force between the SiO_2 microsphere and the gold-coated substrate was measured in ramp mode as a function of the *z*-sensor position (*f*–*z* curve). The adhesive force was determined from the maximum deflection force of the cantilever in the retraction process just before the microsphere left the surface. The *f*–*z* curves were converted to normal force vs. surface separation (*f*–*s*) curves using a conversation method described elsewhere [51]. The lateral stiffness of the cantilever was calibrated by an improved wedge calibration method before each measurement [52, 53]. The friction force was measured by sliding the SiO_2 microsphere perpendicularly to the long axis of the cantilever.

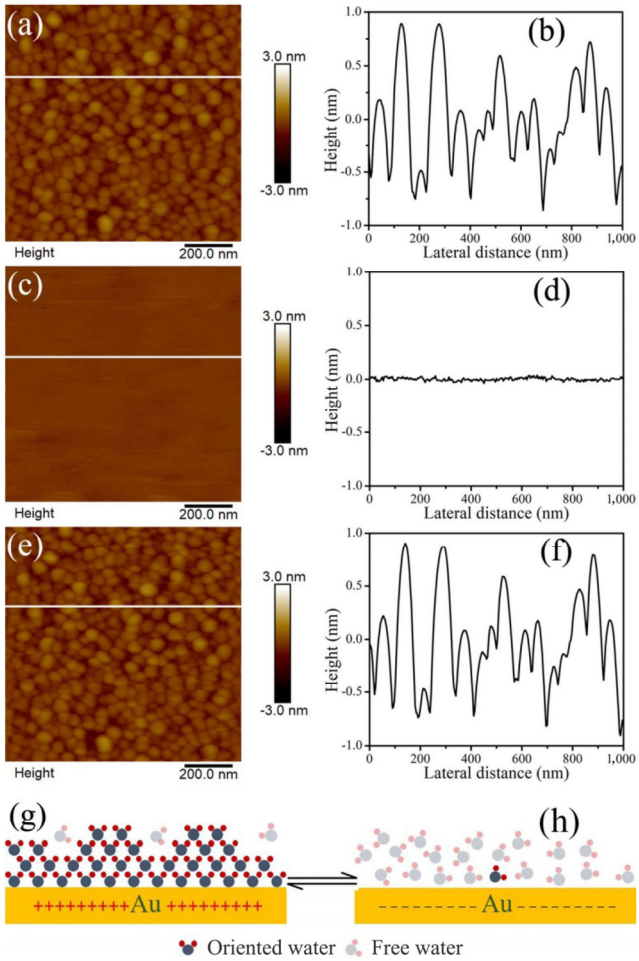

Fig. 1 AFM images of a gold surface at (a) −0.6 V, (c) after increasing to +0.6 V, and (e) after returning to −0.6 V. The scan speed was 500 nm/s. (b), (d), and (f) are height profiles corresponding to the white lines in (a), (c), and (e), respectively. (g) Oriented and (h) free surface water molecules under the influence of positive and negative surface charge, respectively.

3 Results and discussion

The AFM images in Figs. 1(a)–1(c) show the topography of the gold surface when switching between potentials of −0.6 and +0.6 V. The AFM images were prepared using a sharp tip in contact mode with an applied force of 320 nN. When a negative potential of −0.6 V was applied, the surface was rough with some irregular bulges. However, when the potential was increased to +0.6 V, the AFM image portrayed a smooth surface. Then, when the potential was returned to −0.6 V, the surface then returned to its original rough topography. This indicates that the gold surface was not damaged by the sharp tip; rather, at +0.6 V, there was some distance between the gold and the tip that created a flat image. Considering that the double-layer electrostatic force acting on the tip can be neglected (as discussed in our previous study [40, 41]), and that there is a strong hydration effect at +0.6 V (see Fig. 2), we can conclude that a hydration layer exists on the gold surface at +0.6 V that separates the tip from the surface.

To further explore this interfacial hydration layer, normal force curves were obtained at different potentials as the microsphere approached the gold surface (Fig. 2). According to the Derjaguin–Landau–Verwey–Overbeek (DLVO) theory, the microsphere should encounter double-layer electrostatic forces and van der Waals forces as it approaches the gold surface [19, 28]. However, the ionic strength used in our experiments was sufficiently large (0.1 M; corresponding to a Debye length of less than 1 nm) that the electrical double-

layer force may be ignored [28, 40]. In addition, the van der Waals attraction force is not significant for any of the approach curves; thus, the microsphere encounters strong repulsive forces at all surface distances. According to previous studies [19, 27, 28, 32, 40], these repulsive forces can be ascribed to the steric effect of surface-confined water molecules, which is known as hydration force [19]. The effective surface viscosity is relatively low at negative potential because the surface water molecules can move freely [27, 40]; however, as the applied potential increases, the surface water molecules align at the interface to form an ice-like surface layer, increasing the viscosity of the water layer and therefore the repulsion forces [27, 31, 32, 34, 40, 41]. Classical hydrodynamic drainage ($F = 6\pi\eta R^2V/D$) can be used to calculate the viscosity of the surface layer [32, 40, 54, 55]. In the present case, F is the repulsive force acting upon the SiO_2 microsphere; η is the effective viscosity of the surface water layer; R is the radius of the microsphere; V is the approach velocity; and D is the distance between the microsphere and the gold surface. Thus, the effective viscosity of the surface water layer is about 0.05 Pa·s at −0.6 V and about 80 Pa·s at +0.6 V—the latter being five orders of magnitude higher than that of bulk water. These results are in accordance with those of previous studies [32, 39, 54].

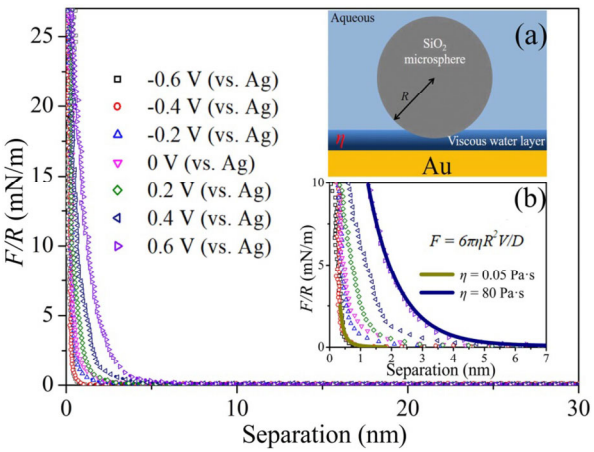

Fig. 2 Normal force curves for SiO_2 microspheres at different separations and electrical potentials in a 0.1 M NaCl solution at an approaching velocity of 500 nm/s. Inset (a) illustrates the surface contact geometry, where η is the viscosity of the surface water layer. Inset (b) shows a magnification of the force curves at separations ranging from 0 to 7 nm. The solid line corresponds to the data obtained at −0.6 and +0.6 V fit assuming a classical hydrodynamic model.

Figure 3 shows the typical friction behavior between the SiO_2 microsphere and the gold surface at positive (+0.6 V) and negative (−0.6 V) potentials. The apparent CoF (defined as the ratio of friction force to normal load) was much higher at positive potential than that at negative potential, as shown in Fig. 3(c). At −0.6 V, the apparent CoF was below 0.01, which is in the range of superlubricity [56, 57]; whereas at +0.6 V, the apparent CoF was approximately 0.035. This change in friction behavior is due to the differences in the confined water structure [38–41]. The ice-like water layer that exists at positive potential is capable of forming hydrogen bonds with the SiO_2 microsphere, resulting in a high CoF [39–41]. However, the ice-like structure is disrupted at negative potential [27, 39, 40, 58], and the aqueous salt solution acts as a boundary lubricant, reducing the attractive forces between the SiO_2 microsphere and gold surface [40, 41] and reducing the CoF [39–41]. Furthermore, as the gold surface is rough at negative potential and smooth at positive potential (see Fig. 1), the actual contact area between the gold surface and the microsphere would be smaller at negative potential, which may also contribute to lower friction.

It is worth noting that a superlubricious state is observed, which is different from the low-friction state that was observed previously at negative potential for the same electrochemical system [40, 41], because the hydration force (shown in Fig. 2) arising from the aqueous salt solution plays a more important role in reducing friction at negative potential. Previously [40], friction switching was observed with a relatively large load on the gold surface (micronewton magnitude) and a sharp AFM tip (radius of curvature: ~10 nm). The CoF was low at negative potential due to the lubrication of the salt solution [39–41] and the disappearance of the structured water. However, the salt solution at the interface was easily removed upon contact because of the high hertzian contact pressure (>21 GPa); therefore, the lubrication effect could not be fully exerted. In contrast, the SiO_2 microsphere used in this study had a larger size (radius: ~10 μm) and was applied at a smaller load (nanonewton magnitude; the maximum Hertzian contact pressure was about 110 MPa), causing the salt solution to create a better hydration lubrication effect at −0.6 V. In

addition, the adhesion between the microsphere and the gold surface is very small at negative potential (less than 1 nN, see Figs. S1 and S2 in the Electronic Supplementary Material (ESM)), which indicates that the interfacial reaction between the microspheres and the gold substrate is extremely weak [59, 60]. These factors promote the occurrence of superlubricity. Figure 3(d) shows the load dependence of the friction force at −0.6 and +0.6 V. A linear relationship was observed at −0.6 V, while a nonlinear relationship was observed at +0.6 V. Notably, this transition was fully reversible upon alternating between −0.6 and +0.6 V several times, with excellent repeatability.

Owing to the highly viscous water layer that forms on the positively charged gold surface, it is possible that the nonlinear behavior observed at +0.6 V is caused by hydrodynamic drag acting on the microsphere in the lateral direction. To investigate this further, the load dependence of the friction force between a polystyrene microsphere and a gold-coated substrate was examined at −0.6 and +0.6 V (Fig. S3 in the ESM). Using the polystyrene microsphere, the friction force was almost the same at +0.6 V as at −0.6 V, and a linear relationship was observed between the friction force and load, irrespective of the potential. This indicates that drag force is unlikely to be the reason for the nonlinear friction behavior observed for the SiO_2 microsphere at positive potential. In addition, such drag forces tend to increase as the sliding speed increases [61, 62]; however, the friction force was observed to decrease with sliding speed (see Fig. S4 in the ESM), further implying that drag contributes little to the friction between the SiO_2 microsphere and positively charged gold surface. A detailed explanation of this decrease in friction with sliding speed is given in the ESM.

The oriented water molecules on the positively charged gold surface create a contact plane with a large number of exposed dangling hydroxyl groups. These hydroxyl groups partake in hydrogen bonding with the hydroxyl groups on the SiO_2 microsphere, leading to high adhesion [27, 40, 41, 63]. Adhesion plays an important role in nanoscale friction, with friction generally increasing with adhesion forces [64, 65]. Nanoscale friction is linearly correlated with load for weak adhesion between two surfaces [66, 67].

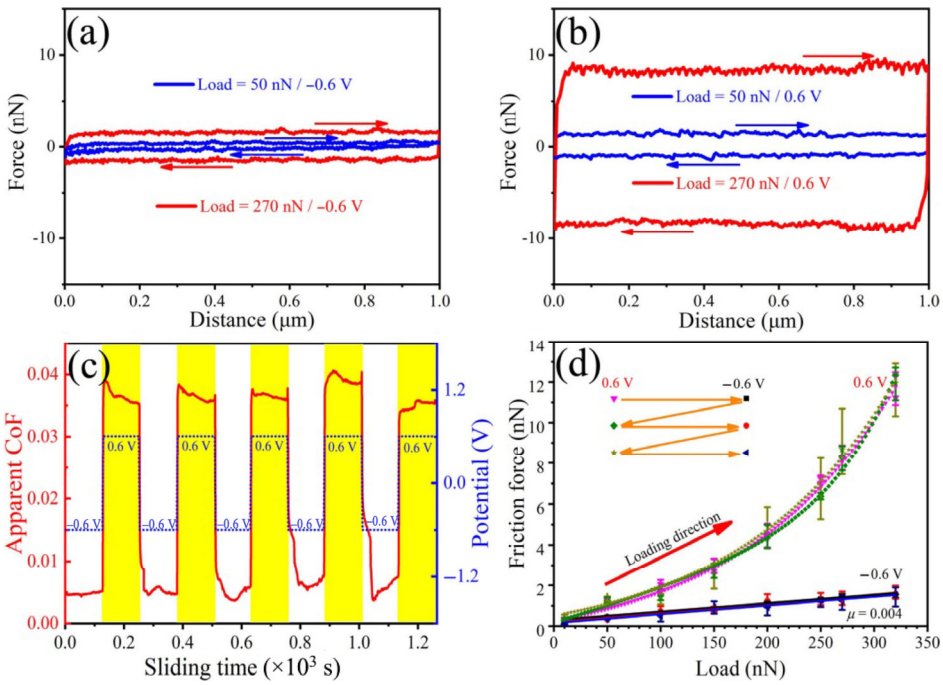

Fig. 3 Friction forces between a SiO_2 microsphere and a gold surface in 0.1 M aqueous NaCl measured at different loads and electrical potentials. Force loops at potentials of (a) −0.6 and (b) +0.6 V. (c) Apparent coefficient of friction (CoF) when the applied potential was alternated between −0.6 and +0.6 V during sliding friction at a load of 320 nN. (d) Multiple cycling test results. Load-dependent friction at high (+0.6 V) and low (−0.6 V) potentials with a sliding velocity of 2 μm/s. The order in which the experiments were performed is shown in the inset.

However, the correlation changes from linear to nonlinear as the adhesion forces increase [66, 67]. Thus, it is necessary to explore the effect of adhesion on friction.

Figure 4(b) shows that at positive potential, the relationship between friction and adhesion is linear as the load increases. At negative potential, the adhesion and friction forces were small, as shown in Figs. S1(a), S2(a), and S2(b) in the ESM. The results indicate that adhesion plays an important role in nonlinear friction at positive potential. Accordingly, we analyzed the friction at positive potential using the classical binomial law of friction (Eq. (1)), which describes friction in terms of the mechanical resistance and molecular attraction [66, 67]. Considering the load dependence, the friction force F_f takes the form

$$F_f = \alpha A + \mu F_L \tag{1}$$

where F_L is the normal load, A is the actual contact area, and μ is a constant representing load dependence. The physical meaning of α was clarified by Israelachvili [28]; it represents the contribution of the adhesive hysteresis $\Delta\gamma$ and its linearly with α. In this work, the adhesion hysteresis is high (see the approach and retraction curves in Fig. S1(b) in the ESM); hence, the adhesive hysteresis is approximately equal to the adhesive interaction strength of the retraction curve ($\Delta\gamma \approx \gamma_R$). Therefore, the friction force takes the form $F_f = k\gamma_R A + \mu F_L$, where k is a constant. For random rough surface contact, the measured adhesive force F_{adh} is considered to be linear with the actual contact area A and the adhesive interaction strength γ_R. It follows that

$$F_f = CF_{adh} + \mu F_L \tag{2}$$

As a result, the friction force is dependent on both the normal load F_L and the adhesive force F_{adh}. The relationship between the adhesive force and load at positive potential is shown in Fig. S1(a) in the ESM, and the relational expression is given in the supplementary information (Eq. (S1) in the ESM). Combining Eqs. (1) and (S1) yields

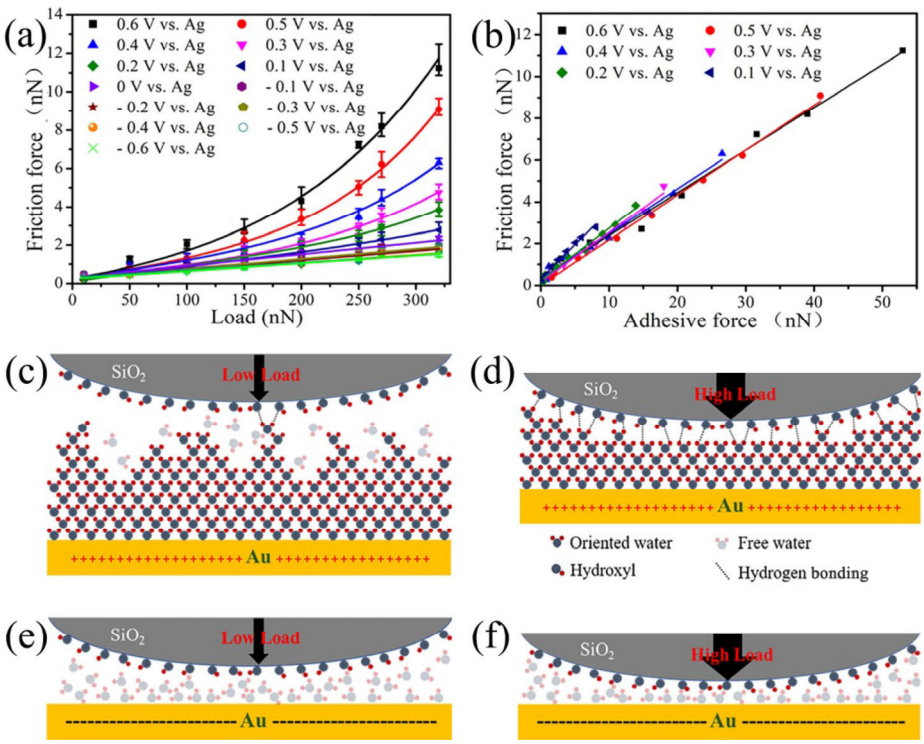

Fig. 4 Load dependence and underlying mechanism of friction behavior at different potentials. (a) Friction force as a function of load at different applied potentials. The nonlinear lines were fitted using Eq. (3). (b) Relationship between friction force and adhesive force at different loads and different positive potentials. (c) At positive potential, when the load is small, few hydrogen bonds can form. (d) When the load is high, a large number of hydrogen bonds form at the contact interface. (e, f) At negative potential, the oriented structure is disrupted and the free water molecules function as a lubricant, resulting in extremely low friction forces.

$$F_f = K \cdot \exp(bF_L) + \mu F_L \quad (3)$$

where b is the attenuation factor of the nonlinear adhesion behavior. By substituting a load of $F_L = 0$ into Eq. (3), the friction force F_f equals to K. Therefore, K represents the strength of adhesion-dominated friction caused by hydrogen bonding [41], which is related with the electric field-induced water structure. The friction data taken at positive potentials in Fig. 4(a) were fitted using Eq. (3), and the fitting parameters are given in Table S1 in the ESM. The values of R^2 are close to 1, indicating that Eq. (3) agrees well with the experimental data.

The extremely low adhesive forces and friction forces at negative potentials (see Fig. S2 in the ESM) indicate that adhesion contributes little to friction in this state. The high adhesion and friction forces at positive potentials are coupled with extremely low μ values (below 0.01, as shown in Table S1 in the ESM), indicating that the high friction at positive potential originates almost completely from the high adhesive force. The values of the dynamic parameters K and b decrease with decreasing potential, indicating a decrease in hydrogen bonding strength, which is consistent with previous studies [40, 41].

Previous studies have revealed that the adhesion between a SiO_2 microsphere and a positively charged gold surface in an aqueous solution originates from hydrogen bonding between the SiO_2 microsphere and the interfacial confined ice-like water layer [27, 40, 41, 63]. By analyzing the adhesion results at positive potential (Figs. 4(b) and S1(a) in the ESM), it is reasonable to infer that hydrogen bonding becomes exponentially weaker with distance from the gold-coated substrate. The high confinement of the interfacial water layer originates from the alignment of water molecules [27, 68]. The population of oriented water molecules is highest adjacent to the positively charged gold surface, and decreases with distance from the surface into the bulk solution [40, 41]. When the SiO_2 microsphere penetrates into the viscous water layer, a high number of oriented water molecules form strong hydrogen bonds with the microsphere. In contrast, when the SiO_2 microsphere is suspended close to (but not in) the viscous water layer, the number of oriented water molecules it encounters is so low that little hydrogen bonding occurs. Based on analysis of the adhesion results (Figs. 4(b) and S1(a) in the ESM), a reasonable inference is that the hydrogen bonding becomes exponentially weaker with distance from the gold-coated substrate. This nonlinear decay of hydrogen bonding would become more pronounced with increasing potential, because the surface water molecules align to a greater extent at higher potentials [27, 40, 68], resulting in a larger difference in the number of oriented water molecules between the surface and bottom of the confined water layer.

Thus, the nonlinearity of the friction behavior with increasing load on the positively charged gold surface can be attributed to the strength of hydrogen bonding at the contact interface. When the loading force is low (10 nN), hydrogen bonding at the contact interface is so weak that the attraction between the SiO_2 microsphere and the gold-coated substrate contributes little to interfacial friction, as shown in Fig. 4(c). Upon increasing the loading force, the contact interface is forced closer to the gold-coated substrate, where the hydrogen bonding becomes exponentially stronger (Fig. 4(d)). This strong hydrogen bonding causes the friction force to increase rapidly, resulting in nonlinear friction behavior with load. Conversely, under negative potential, the oriented water structure is disrupted, preventing hydrogen bonding between the SiO_2 and the surface water layer. The free water adsorbed at the Au/SiO_2 interface bears the nanonewton scale normal load, and acts as an effective boundary lubricant, resulting in a superlubricious state that has a linear correlation with load, as shown in Figs. 4(e) and 4(f). Since the transition of the water structure under positive and negative potential is reversible [27, 40, 41], the transition of friction is also reversible.

Owing to the lubrication mechanism, the reversible switching of the lubrication state and nonlinear friction behavior is not limited to systems using aqueous NaCl solution. Similar friction and lubrication behaviors were observed with NaOH, KCl, and $NaNO_3$ aqueous solutions (see Fig. S5 in the ESM). Thus, this study may have a far-reaching impact on many important fields of science and technology related to friction, adhesion, and wear. For example, it is difficult to precisely control the lifetime of M/NEMSs, because control of the friction state with very small dimensions and loads and high surface area-to-volume ratios is required [26].

The system explored in the present study demonstrates that appropriate electrical stimulation can precisely alter the interfacial friction behavior. Furthermore, this approach has good durability (Fig. S6 in the ESM). In addition, aqueous salt solutions are good conductive lubricants for contacting electrified surfaces [69, 70]. Traditional oil lubricants or molecular lubricants such polytetrafluoroethylene are not suitable for such situations because of their electrical insulation properties.

4 Conclusions

We demonstrated the reversible switching between superlubricity and nonlinear high friction of a gold surface sliding against a SiO_2 microsphere in aqueous solution by tuning the electrochemical potential. At a negative potential, the apparent CoF was lower than 0.01, which is in the range of superlubricity; the friction force changed linearly with load, in accordance with Amonton's law. Conversely, at positive potential, the apparent CoF was higher, and the friction force increased nonlinearly with load. A relationship between external load, interfacial adhesion, and friction at positive potentials was developed, which indicates that the nonlinear high friction is caused by the strength of hydrogen bonding at the shearing plane. Thus, our findings constitute an advancement in the theory of potential-controlled friction between surfaces. This may have far-reaching implications for the development of nanotechnologies for use in M/NEMSs.

Acknowledgements

This work was supported by the National Natural Science Foundation of China (Nos. 51901112 and 51425502), China Postdoctoral Science Foundation (No. 2018M630145) and the Major Scientific Research and Development Project in Jiangxi (No. 20173ABC28008). We thank Xiaosong Li and Xinxin Li in our research group for the design of graphics.

Electronic Supplementary Material: Supplementary materials (load-dependent adhesive force at different potentials; friction and adhesive force at negative potentials; friction behavior between a polystyrene (PS) microsphere and the charged gold surface; friction force vs. sliding velocity at −0.6 and +0.6 V; lubrication state and friction behavior in NaOH, KCl, and $NaNO_3$ aqueous solutions; apparent CoF versus the repeat cycle) are available in the online version of this article at https://doi.org/10.1007/s40544-019-0354-7.

References

[1] Merkle A P, Marks L. A predictive analytical friction model from basic theories of interfaces, contacts and dislocations. *Tribol Lett* **26**(1): 73–84 (2007)

[2] Bowden F P, Tabor D. *Friction and Lubrication of Solids*. Oxford (UK): Oxford University Press, 1950.

[3] Rabinowicz, E, Tanner R I. Friction and wear of materials. *J Appl Mech* **33**(2): 479–479 (1966)

[4] Labuda A, Hausen F, Gosvami N N, Grütter P, H, Lennox R, B, Bennewitz R. Switching atomic friction by electrochemical oxidation. *Langmuir* **27**(6): 2561–2566 (2011)

[5] Kawai, S.; Sasaki, N.; Kawakatsu, H. Direct mapping of the lateral force gradient on Si (111)-7 × 7. *Phys Rev B* **79**(19): 195412 (2009)

[6] Hoshi Y, Kawagishi T, Kawakatsu H. Velocity dependence and limitations of friction force microscopy of mica and graphite. *Jpn J Appl Phys* **39**(1): 3804–3807 (2000)

[7] Sahin M, Cetinarslan C S, Akata H E. Effect of surface roughness on friction coefficients during upsetting processes for different materials. *Mater Des* **28**(2): 633–640 (2007)

[8] Ghabrial S R, Zaghlool S A. The effect of surface roughness

on static friction. *Int J Machine Tool Des Res* **14**(4): 299–309 (1974)

[9] Zhao Z, Yang X, Li S, Li D. Interfacial bonding features of friction stir additive manufactured build for 2195-T8 aluminum-lithium alloy. *J Manuf Proc* **38**: 396–410 (2019)

[10] Li A, Liu Y, Szlufarska I. Effects of interfacial bonding on friction and wear at silica/silica interfaces. *Tribol Lett* **56**(3): 481–490 (2014)

[11] Wolloch M, Levita G, Restuccia P, Righi M. Interfacial charge density and its connection to adhesion and frictional forces. *Phys Rev Lett* **121**(2): 026804 (2018)

[12] Sun J, Zhang Y, Lu Z, Li Q, Xue Q, Du S, Pu J, Wang L. Superlubricity enabled by pressure-induced friction collapse. *J Phys Chem Lett* **9**(10): 2554–2559 (2018)

[13] Gropper D, Wang L, Harvey T J. Hydrodynamic lubrication of textured surfaces: a review of modeling techniques and key findings. *Tribol Int* **94**: 509–529 (2016)

[14] Zhang J, Meng Y. Boundary lubrication by adsorption film. *Friction* **3**(2): 115–147 (2015)

[15] Briscoe W H, Titmuss S, Tiberg F, Thomas R K, Mcgillivray D J, Klein J. Boundary lubrication under water. *Nature* **444**(7116): 191–194 (2006)

[16] Hills B A, Boundary lubrication *in vivo*. *Inst Mech Eng Part H* **214**(1): 83–94 (2000)

[17] Patir N, Cheng H S. An average flow model for determining effects of three-dimensional roughness on partial hydrodynamic lubrication. *J Lubr Technol* **100**(1): 12–17 (1978)

[18] Hamrock B J, Dowson D. Isothermal elastohydrodynamic lubrication of point contacts: Part III—Fully flooded results. *J Lubr Technol* **99**(2): 264–275 (1977)

[19] Klein J. Hydration Lubrication. *Friction* **1**(1): 1–23 (2013)

[20] Persson K, Gahlin R. Tribological performance of a DLC coating in combination with water-based lubricants. *Tribol Int* **36**(11): 851–855 (2003)

[21] Deng M, Li J, Zhang C, Ren J, Zhou N, Luo J. Investigation of running-in process in water-based lubrication aimed at achieving super-low friction. *Tribol Int* **102**: 257–264 (2006)

[22] Karuppiah K S K, Zhou Y, Woo L K. Sundararajan S. Nanoscale friction switches: friction modulation of mono-molecular assemblies using external electric fields. *Langmuir* **25**(20): 12114–12119 (2009)

[23] Lahann J, Mitragotri S, Tran T N, Kaido H, Sundaram J, Choi I S. Hoffer S, Somorjai G A, Langer R. A reversibly switching surface. *Science* **299**(5605): 371 (2003)

[24] Binggeli M, Christoph R, Hintermann H E, Colchero J, Marti O. Friction force measurements on potential controlled graphite in an electrolytic environment. *Nanotechnology* **4**(2): 59–63 (1993)

[25] Strelcov E, Kumar R, Bocharova V, Sumpter B G, Tselev A, Kalinin S V. Nanoscale lubrication of ionic surfaces controlled via a strong electric field. *Sci Rep* **5**(1): 8049–8049 (2015)

[26] Sweeney J, Hausen F, Hayes R, Webber G B, Endres F, Rutland M W, Bennewitz R, Atkin R. Control of nanoscale friction on gold in an ionic liquid by a potential-dependent ionic lubricant layer. *Phys Rev Lett* **109**(15): 155502 (2012)

[27] Velasco-Velez J J, Wu C H, Pascal T A, Wan L F, Guo J, Prendergast D, Salmeron M. The structure of interfacial water on gold electrodes studied by X-ray absorption spectroscopy. *Science* **346**(6211): 831–834 (2014)

[28] Israelachvili J N. *Intermolecular and Surface Forces*. Academic Press, 2011.

[29] Khan S H, Matei G, Patil S. Hoffmann P M. Dynamic solidification in nanoconfined water films. *Phys Rev Lett* **105**(10): 106101 (2010)

[30] Kim H I, Kushmerick J G, Houston J E, Bunker B C. Viscous "interphase" water adjacent to oligo(ethylene glycol)-terminated monolayers. *Langmuir* **19**(22): 9271–9275 (2003)

[31] Plausinaitis D, Pulmanas A, Kubilius V, Raudonis R, Daujotis V. Properties of an interfacial solution layer at gold electrode surface in perchlorate and chloride solutions: piezoelectric resonator and drag force study. *Electrochim Acta* **121**: 278–284 (2014)

[32] Guriyanova S, Mairanovsky V G, Bonaccurso E. Super-viscosity and electroviscous effects at an electrode/aqueous electrolyte interface: An atomic force microscope study. *J Colloid Interface Sci* **360**(2): 800–804 (2011)

[33] Raviv U, Klein J. Fluidity of bound hydration layers. *Science* **297**(5586): 1540 (2002)

[34] Antognozzi M, Humphris A D L, Miles M J. Observation of molecular layering in a confined water film and study of the layers viscoelastic properties. *Appl Phys Lett* **78**(3): 300–302 (2001)

[35] Dhinojwala A, Granick S. Relaxation time of confined aqueous films under shear. *J Am Chem Soc* **119**(1): 241–242 (1997)

[36] Toney M F, Howard J N, Richer J, Borges G L, Gordon J G, Melroy O R, Wiesler D G, Yee D, Sorensen L B. Voltage-dependent ordering of water molecules at an electrode–electrolyte interface. *Nature* **368**(6470): 444 (1994)

[37] Lee S H, Rossky P J. A comparison of the structure and dynamics of liquid water at hydrophobic and hydrophilic surfaces—a molecular dynamics simulation study. *J Chem Phys* **100**(4): 3334–3345 (1994)

[38] Dhopatkar N, Defante A P, Dhinojwala A. Ice-like water supports hydration forces and eases sliding friction. *Sci Adv* **2**(8): e1600763 (2016)

[39] Valtiner M, Banquy X, Kristiansen K, Greene G W. Israelachvili J N. The electrochemical surface forces apparatus: The effect of surface roughness, electrostatic surface potentials, and anodic oxide growth on interaction forces, and friction between dissimilar surfaces in aqueous solutions. *Langmuir*

28(36): 13080–13093 (2012)

[40] Pashazanusi L, Oguntoye M, Oak S, Albert J N L, Pratt L R, Pesika N S. Anomalous potential-dependent friction on Au(111) measured by AFM. *Langmuir* **34**(3): 801–806 (2018)

[41] Li S, Bai P, Li Y, Chen C, Meng Y, Tian Y. Electric potential-controlled interfacial interaction between gold and hydrophilic/hydrophobic surfaces in aqueous solutions. *J Phys Chem C* **122**(39): 22549–22555 (2018)

[42] Yang X, Meng Y, Tian Y. Potential-controlled boundary lubrication of stainless steels in non-aqueous sodium dodecyl sulfate solutions. *Tribol Lett* **53**(1): 17–26 (2014)

[43] He S, Meng Y, Tian Y. Correlation between adsorption/desorption of surfactant and change in friction of stainless steel in aqueous solutions under different electrode potentials. *Tribol Lett* **41**(3): 485–494 (2011)

[44] Li H, Wood R J, Rutland M W, Atkin R. An ionic liquid lubricant enables superlubricity to be "switched on" in situ using an electrical potential. *Chem Commun* **50**(33): 4368–4370 (2014).

[45] Zhao Y, Wu Y, Wang L, Zhang M, Chen X, Liu M, Fan J, Liu J, Zhou F, Wang Z. Bio-inspired reversible underwater adhesive. *Nat Commun* **8**(1): 2218 (2017)

[46] Wu Y, Wei Q, Cai M, Zhou F. Interfacial Friction Control. *Adv Mater Interfaces* **2**(2): 1400392 (2015)

[47] Wu Y, Cai M, Pei X, Liang Y, Zhou F. Switching friction with thermal-responsive gels. *Macromol. Rapid Commun* **34**(22): 1785–1790 (2013)

[48] Sader J E, Sanelli J A, Adamson B D, Monty J P, Wei X, Crawford S A, Friend J R, Marusic I, Mulvaney P, Bieske E J. Spring constant calibration of atomic force microscope cantilevers of arbitrary shape. *Rev Sci Instrum* **83**(10): 103705 (2012)

[49] Sader J E, Chon J W, Mulvaney P. Calibration of rectangular atomic force microscope cantilevers. *Rev Sci Instrum* **70**(10): 3967–3969 (1999)

[50] Sader J E, Larson I, Mulvaney P, White L R. Method for the calibration of atomic force microscope cantilevers. *Rev Sci Instrum* **66**(7): 3789–3798 (1995)

[51] Ducker W A, Senden T J, Pashley R M. Measurement of forces in liquids using a force microscope. *Langmuir* **8**(7): 1831-1836 (1992)

[52] Li J, Zhang C, Cheng P, Chen X, Wang W, Luo J. AFM studies on liquid superlubricity between silica surfaces achieved with surfactant micelles. *Langmuir* **32**(22): 5593–5599 (2016)

[53] Varenberg M, Etsion I, Halperin G. An improved wedge calibration method for lateral force in atomic force microscopy. *Rev Sci Instrum* **74**(7): 3362–3367 (2003)

[54] Feibelman P J. Effect of high-viscosity interphases on drainage between hydrophilic surfaces. *Langmuir* **20**(4): 1239–1244 (2004)

[55] Chan D Y C, Horn R G. The drainage of thin liquid films between solid surfaces. *J Chem Phys* **83**(10): 5311–5324 (1985)

[56] Li J, Luo J. Advancements in superlubricity. *Sci China: Technol Sci* **56**(12): 2877–2887 (2013)

[57] Li J, Zhang C, Luo J. Superlubricity behavior with phosphoric acid–water network induced by rubbing. *Langmuir* **27**(15): 9413–9417 (2011)

[58] Ataka K I, Yotsuyanagi T, Osawa M. Potential-dependent reorientation of water molecules at an electrode/electrolyte interface studied by surface-enhanced infrared absorption spectroscopy. *J Phys Chem* **100**(25): 10664–10672 (1996)

[59] Myshkin N, Kovalev A. Adhesion and surface forces in polymer tribology—A review. *Friction* **6**(2): 143–155 (2018)

[60] Zhou M, Pesika N, Zeng HB, Tian Y, Israelachvili J. Recent advances in gecko adhesion and friction mechanisms and development of gecko-inspired dry adhesive surfaces. *Friction* **1**(2): 114–129 (2013)

[61] Mechler Á, Piorek B, Lal R, Banerjee S. Nanoscale velocity–drag force relationship in thin liquid layers measured by atomic force microscopy. *Appl Phys Lett* **85**(17): 3881–3883 (2004)

[62] Toussaint H, De Groot G, Savelberg H, Vervoorn K, Hollander A, van Ingen Schenau G. Active drag related to velocity in male and female swimmers. *J Biomech* **21**(5): 435–438 (1988)

[63] Chen J, Ratera I, Park J Y, Salmeron M. Velocity dependence of friction and hydrogen bonding effects. *Phys Rev Lett* **96**(23): 236102 (2006)

[64] Zeng X, Peng Y, Yu M, Lang H, Cao X A, Zou K. Dynamic sliding enhancement on the friction and adhesion of graphene, graphene oxide, and fluorinated graphene. *ACS Appl Mater Interfaces* **10**(9): 8214–8224 (2018)

[65] Ando Y, Tanaka T, Ino J, Kakuta K. Relationships of friction, pull-off forces and nanometer-scale surface geometry. *JSME Int J Ser* **44**(2): 453–461 (2001)

[66] Elinski M B, Menard B D, Liu Z, Batteas J D. Adhesion and friction at graphene/self-assembled monolayer interfaces investigated by atomic force microscopy. *J Phys Chem C* **121**(10): 5635–5641 (2017).

[67] Gao J, Luedtke W D, Gourdon D, Ruths M, Israelachvili J N, Landman U. Frictional forces and Amontons' Law: From the molecular to the macroscopic scale. *J Phys* Chem *B* **108**(11): 3410–3425 (2004)

[68] Noguchi H, Okada T, Uosaki K. SFG study on potential-dependent structure of water at Pt electrode/electrolyte solution interface. *Electrochim Acta* **53**(23): 6841-6844 (2008)

[69] Horn R G, Smith D T. Contact electrification and adhesion between dissimilar materials. *Science* **256**(5055): 362–364 (1992)

[70] Shah J, Hahn W. Material characterization of thick film resistor pastes. *IEEE Trans Compon Hybrids Manuf Technol* **1**(4): 383–392 (1978)

Shaowei LI. He received his Ph.D. degree at China University of Petroleum (Beijing), in 2017, majoring in materials science and engineering. He is currently a post-doctor at the State Key Laboratory of Tribology in Tsinghua University. Dr. LI has published 7 peer-reviewed journal papers. His research interests include the micro-nano mechanics, thermal spray technology, interfacial molecular assembly, and lubricant development, etc.

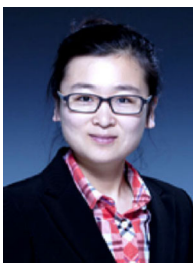

Liran MA. She received her B.S. degree from Tsinghua University in 2005, and received her Ph.D. degree from Tsinghua University in 2010. Following a postdoctoral period at the Weizmann Institute of Science in Israel, she is now working as an associate professor in State Key Laboratory of Tribology, Tsinghua University. Her interests in tribology have ranged from aqueous lubrication and hydration lubrication to the liquid/solid interface properties. She has published over 50 papers. Her honors include the Hinwin Doctoral Dissertation Award (2011), the Maple Leaf Award for Outstanding Young Tribologists (2015), and Chang Jiang Scholars Program-Young Professor Award (2015).

Yu TIAN. He is professor and director of the State Key Laboratory of Tribology at Tsinghua University of China. Tian gained his B.S. and Ph.D. degrees in mechanical engineering at Tsinghua University in 1998 and 2002, respectively. Subsequently he joined the State Key Laboratory of Tribology. He was a postdoc at the University of California, Santa Barbara with Professor Jacob Israelachvili from 2005 to 2007. His research interest is the science and technology at the interface of physics, materials, engineering and biology to understand the physical laws of adhesion, friction and rheology to implement technological inventions to benefit the society. He has published over 150 peer-reviewed journal papers. He has received the Ten Thousand People Leading Plan Innovation Leading Talents of China (2019), the Youth Science and Technology Award of China (2016), the Yangtze River Scholars Distinguished Professor (2015–2019), the National Natural Science Foundation for Distinguished Young Scientists of China (2014), the Wen Shizhu-Maple Award-Young Scholar Award (2012), the Young Scholar Achievement Award of the Society of Mechanical Engineering of China (2011), Outstanding Young Scholar Award of the Chinese Tribology Institute (2009), and the National Excellent Doctoral Dissertation of China (2004).